nature geoscience

LETTERS

PUBLISHED ONLINE: 7 JULY 2013 | DOI: 10.1038/NGEO1863

Imprint of Southern Ocean eddies on winds, clouds and rainfall

I. Frenger[1,2]*, N. Gruber[1,2], R. Knutti[3] and M. Münnich[2]

Owing to the turbulent nature of the ocean, mesoscale eddies are omnipresent. The impact of these transitory and approximately circular sea surface temperature fronts on the overlying atmosphere is not well known. Stationary fronts such as the Gulf Stream have been reported to lead to pronounced atmospheric changes[1,2]. However, the impact of transient ocean eddies on the atmosphere has not been determined systematically, except on winds and to some extent clouds[3–6]. Here, we examine the atmospheric conditions associated with over 600,000 individual eddies in the Southern Ocean, using satellite data. We show that ocean eddies locally affect near-surface wind, cloud properties and rainfall. The observed pattern of atmospheric change is consistent with a mechanism in which sea surface temperature anomalies associated with the oceanic eddies modify turbulence in the atmospheric boundary layer. In the case of cyclonic eddies, this modification triggers a slackening of near-surface winds, a decline in cloud fraction and water content, and a reduction in rainfall. We conclude that transient mesoscale ocean structures can significantly affect much larger atmospheric low-pressure systems that swiftly pass by at the latitudes investigated.

Although the ocean and atmosphere form a closely interacting system, it has generally been assumed that these interactions occur primarily at the synoptic and global scale. At these scales the atmosphere drives the ocean through buoyancy changes and momentum input by winds, and the ocean affects the atmosphere through heat and moisture fluxes[7].

It has been less clear, however, how strongly the ocean and atmosphere interact on the mesoscale, especially in the extra-tropics. What is known is that mesoscale sea surface temperature (SST) anomalies are globally correlated with near-surface winds and albedo[4,6]. Concurrent modifications of winds and clouds were detected for the distinct Gulf Stream rings[5] and for large-scale fronts such as the semi-permanent Agulhas Return Current[8,9]. In addition, an SST-related change of rain rate was observed for the Gulf Stream and the Kuroshio (for example, refs[1,10]).

However, large-scale fronts are outnumbered by mesoscale eddies, which dominate the ocean's kinetic energy[11] and typically feature an SST anomaly[12]. Despite their prevalence, little is known about systematic atmospheric perturbations related to these non-stationary mesoscale SST anomalies. Here we close this gap, and show on the basis of observations how oceanic mesoscale eddies impact the atmosphere by changing not only wind, but also clouds and rainfall.

Our analysis is based on the identification of more than 600,000 oceanic eddies south of 30 °S over a period of more than seven years (June 2002 to November 2009). To identify the oceanic eddies, we applied a standard detection method based on the Okubo–Weiss parameter[13,14] to weekly maps of satellite-derived sea level anomalies (see Method Section for details). For each eddy that was detected at least twice, we collocated satellite-derived SST and atmospheric data (wind speed and direction, cloud fraction, liquid cloud water content, rain rate and rain probability).

Most of the identified eddies are located in the frontal region of the intense Antarctic Circumpolar Current especially in the Indian and Pacific sectors (Fig. 1a) with both cyclonic and anticyclonic eddies occurring in the same regions. We found relatively little seasonality in the number of detected eddies as well as their atmospheric impact (Supplementary Fig. S1). Therefore, we analyse and present only the long-term mean results. The average detected eddy core has a radius of about 40 km, propagates by more than 20 km a week and is characterized by an SST anomaly of about −0.5 °C in the case of a cyclonic (cold-core) eddy, and +0.5 °C in the case of an anticyclonic (warm-core) eddy. These SST anomalies induce a sufficiently large anomalous air–sea heat flux to cause measurable changes in the marine atmospheric boundary layer (Supplementary Note S1).

Indeed, SST anomalies associated with the cyclonic and anticyclonic eddies are positively correlated with anomalies in near-surface wind speed, cloud fraction, cloud water content, rain rate and rain probability throughout the Southern Ocean (Fig. 1b–d and Supplementary Fig. S2). The correlations are highly significant almost everywhere. When computing the significance, we assumed that the weekly composites of the atmospheric quantities were independent—an assumption supported by the short decorrelation timescale of atmospheric quantities over the Southern Ocean (Supplementary Fig. S3).

The positive correlation indicates that the oceanic SST anomalies associated with eddies are responsible for the atmospheric anomalies, and not vice versa, as the latter would tend to lead to negative correlations[7]. The correlation is highest for wind speed and cloud fraction, smaller for cloud water content and the lowest for rain. Further, it is strongest in regions of large SST anomalies, high eddy activity and for high wind speeds (in agreement with ref. 15), and similar for both cyclonic and anticyclonic eddies, indicating a linear effect of the oceanic forcing on the atmosphere (Supplementary Fig. S4).

To investigate the mechanisms underlying this mesoscale oceanic forcing of the atmosphere, we computed mean composites of the spatial pattern of the imprint on the SST and the atmosphere for all identified eddies. To this end, we centred the SST and atmospheric quantities relative to the eddy core, scaled them relative

[1]Center for Climate Systems Modeling (C2SM), ETH Zürich, Universitätstrasse 16, 8092 Zurich, Switzerland, [2]Environmental Physics, Institute of Biogeochemistry and Pollutant Dynamics, ETH Zürich, Universitätstrasse 16, 8092 Zurich, Switzerland, [3]Climate Physics, Institute for Atmospheric and Climate Science, ETH Zürich, Universitätstrasse 16, 8092 Zurich, Switzerland. *e-mail: ivy.frenger@env.ethz.ch

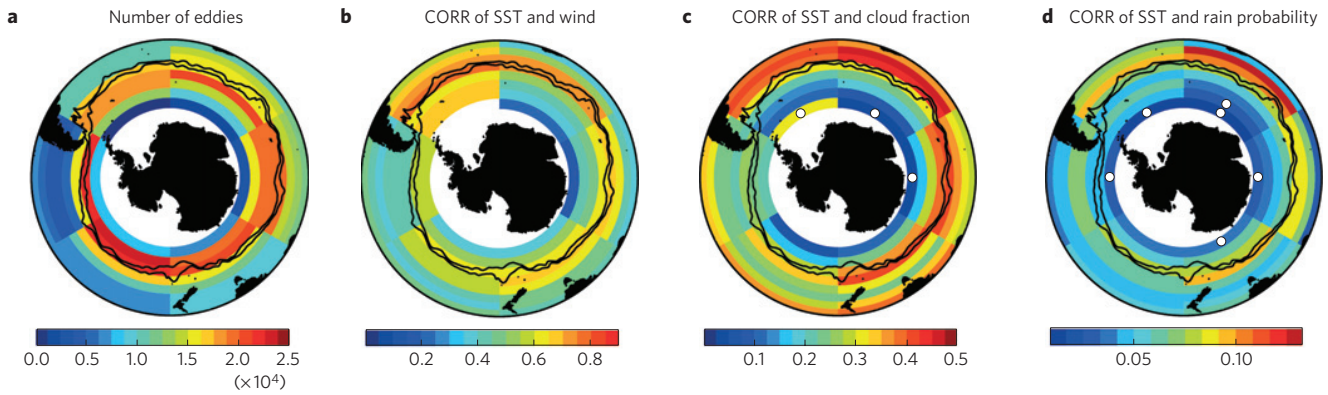

Figure 1 | Polar orthographic maps of the eddy statistics. a–d, Number of detected eddies in each 60° × 4° bin (**a**) and correlations (CORR) of anomalies of SST with anomalies of wind speed (**b**), cloud fraction (**c**) and rain probability (**d**). White dots mark bins where correlations are not significant ($P > 0.01$) and white areas feature insufficient data; black contours denote the two main fronts of the Antarctic Circumpolar Current (the subantarctic and the Polar Front[29]).

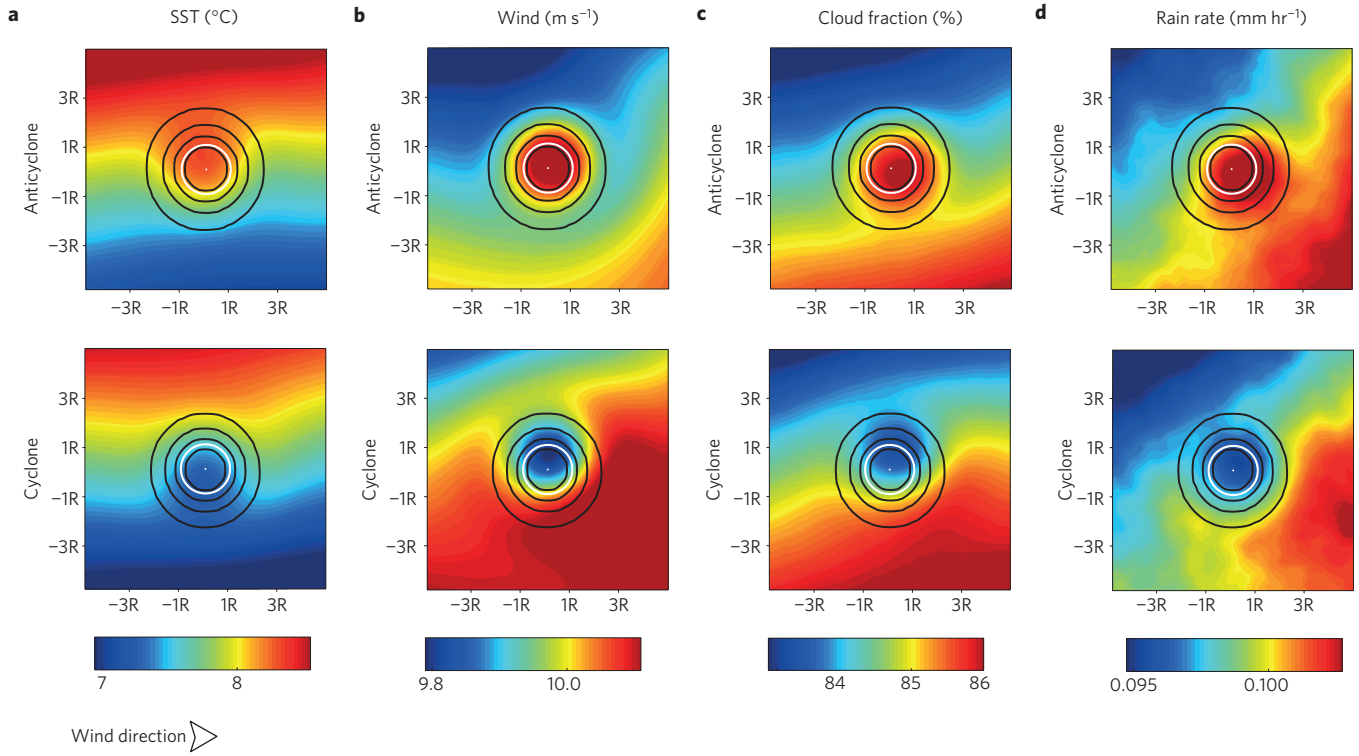

Figure 2 | Mean eddy and pattern of its atmospheric imprint. a, SST (±0.04 °C). **b**, Wind speed (±0.01 ms^{-1}). **c**, Cloud fraction (±0.1%). **d**, Rain rate (±10^{-3} mm h^{-1}). Shown are mean composite maps of the >600,000 individual eddy realizations south of 30 °S, divided into anticyclones and cyclones. White circles mark the eddy core as detected with the Okubo–Weiss parameter and black lines denote sea level anomaly contours associated with the eddy. Before averaging, the eddies were scaled according to their individual eddy amplitude and radius (R), interpolated and rotated so that the large-scale wind is from left to right.

to the individual eddy radius, and rotated them according to the present large-scale wind direction.

A smooth picture of the mean impact of oceanic eddies on the atmosphere emerges, with the anomalies related to the eddy cores distinctly standing out from the background (Fig. 2 and Supplementary Fig. S5). This background largely reflects the large-scale north–south gradients, as the winds are predominantly westerly at these latitudes. In view of the tight spatial coupling and the similar circular shape of the atmospheric response and the SST anomalies (not shown) associated with the eddies, we conclude that we detected a direct response of the atmosphere to SST anomalies of ocean eddies and not to the large-scale SST fronts these eddies are frequently embedded in. The pattern of the atmospheric imprint by the oceanic eddies is nearly symmetric between the cyclonic and anticyclonic eddies but of opposite sign, and the maximum radial extent of the imprint corresponds roughly to 2–3 eddy-core radii (80–120 km).

The atmospheric imprints are well quantifiable, and although of moderate magnitude relative to the mean state (2–5%), they are statistically significant (Kolmogorov–Smirnov test, $p = 0.01$). Anticyclonic and cyclonic eddies cause maximum positive and negative anomalies (see Methods), respectively, with maximum mean anomalies of wind of 0.31 ± 0.01 m s^{-1}, of cloud fraction of 1.7 ± 0.1%, of cloud water content of

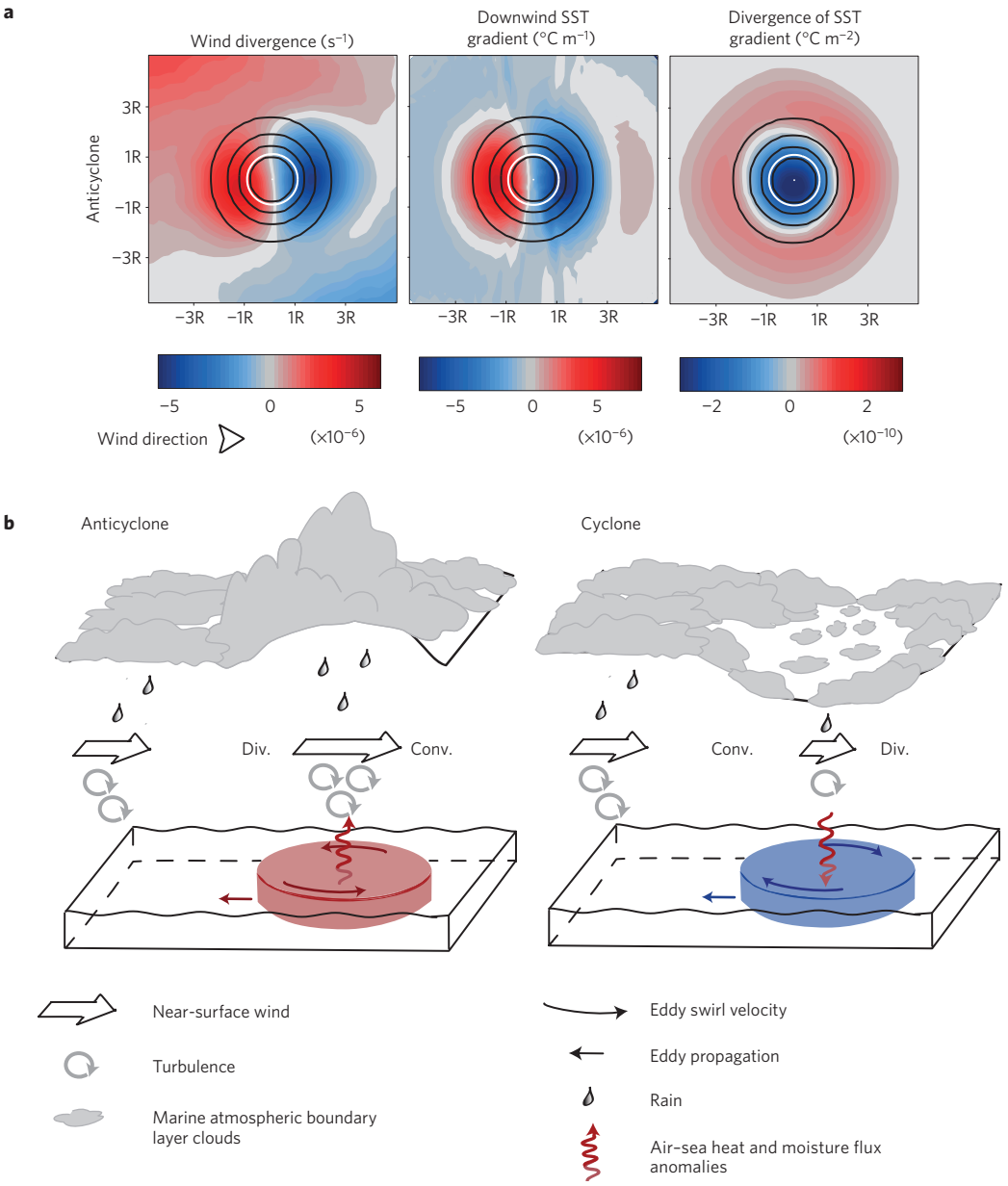

Figure 3 | Impact of mesoscale oceanic eddies on the atmosphere. a, Mean composite of the wind divergence (left), downwind SST gradient (middle) and divergence of the SST gradient, that is, the Laplacian of the SST (right). The graph is very similar but of opposite sign for cyclonic eddies (not shown). Otherwise as Fig. 2. **b**, Schematic summarizing the impact of oceanic eddies on the lower atmosphere for a Southern Hemispheric warm-core anticyclone (red, left) and a cold-core cyclone (blue, right). Div., wind divergence; conv., wind convergence.

$2.9 \pm 0.3 \times 10^{-3}$ mm, of rain rate of $4 \pm 1 \times 10^{-3}$ mm h^{-1} and of rain probabilities of 1.7±0.3%. Relative to the atmospheric variability, the magnitude of these anomalies represents 13–15% (wind, cloud fraction), 6–10% (cloud water content) and 2–6% (rain).

Two main mechanisms, downward momentum transport and pressure adjustment, have been proposed to explain the adjustments in the atmosphere resulting from SST gradients[16,17]. The former relates to a decrease of the vertical stability of the atmosphere as air moves from cold to warm water. This leads to an intensification of the turbulence within the atmospheric boundary layer and thus an increased downward momentum transport. Subsequently, the near-surface vertical wind shear is increased and the near-surface wind intensifies centred over the SST anomaly. The pressure adjustment mechanism relates to changes of the near-surface air density and thus of the sea level pressure. Here, negative sea level pressure anomalies arise over a warm SST anomaly from modified air–sea fluxes, yielding an acceleration of wind upstream of the warm SST anomaly and a deceleration downstream of it. Which mechanism is dominant can be estimated from the spatial pattern of the SST in combination with the wind divergence (Fig. 3a). In the case of the pressure adjustment mechanism, one expects a monopole pattern corresponding to the divergence of the SST gradient[2], as the surface wind converges over a positive SST anomaly. In contrast, one expects a dipole pattern for the downwind momentum transport mechanism[4]. This is because the wind speed increase over the SST anomaly is accompanied by a wind divergence upstream and a convergence downstream of the SST anomaly, and hence it has the same structure as the dipole-shaped downwind gradient of SST.

The resemblance of the wind divergence and the downwind SST gradient in Fig. 3a favours the downwind momentum

mixing mechanism as an explanation. This implies that the perturbed air–sea fluxes associated with the steep gradients of the SST upstream and downstream of the eddy core lead to the changes in the near-surface wind by changing the turbulent mixing in the atmospheric boundary layer, as anticipated under conditions of strong cross-frontal winds[15] (Fig. 3b). Similarly, the nearly in-phase relationship of cloud and rain anomalies with those of SST and wind speed points to a modification of the atmospheric boundary layer stability and hence convection (enhancement/suppression) in combination with changes in the moisture supply as the likely cause, in contrast to vertical air motion triggered by the wind divergence/convergence. Thus, the thermodynamical and dynamical adjustments in the marine atmospheric boundary layer due to the eddies' SST anomalies become apparent in a modification of local weather. These modifications are presumably accompanied by a change of the atmospheric boundary layer height[16] but probably remain restricted to the atmospheric boundary layer.

The mesoscale modifications of the atmosphere related to oceanic eddies represent yet another piece of the puzzle of the energy and hydrological cycle of the Earth system. Southern Ocean eddies provide a source of atmospheric variability in the latitudes of the prevailing westerlies in the Southern Hemisphere at spatial scales of $O(100)$ km. We thus suggest to incorporate this additional SST variability in numerical weather prediction models to improve their skill[18]. The subsequent feedbacks of the atmosphere on the ocean may be of significance for ocean dynamics including the mesoscale eddy field[19]. First, changes of the wind stress curl due to SST anomalies are directly related to upwelling and suction in the surface ocean. Second, changes in wind speed as well as cloud fraction constitute negative feedbacks by damping the SST anomalies and potentially leading to an acceleration of eddy dissipation[20]. Third, and in contrast to the above, the eddy-induced changes of rainfall could constitute a positive feedback: in the case of anticyclonic eddies, the increased freshwater input decreases further the low-density anomaly, and vice versa for cyclonic eddies.

Mesoscale eddy-induced atmospheric responses might also be relevant for ocean biogeochemistry, especially for the oceanic uptake of carbon dioxide (CO_2). For cold-core cyclonic eddies, for which the partial pressure of CO_2 (p_{CO_2}) is ~2% lower than that of the surrounding waters, a ~4% lower gas transfer rate due to the concurrent attenuated winds leads to a reduction of the anomalous sink associated with these eddies. In contrast, in the case of the warm-core anticyclonic eddies, whose p_{CO_2} tends to be higher than that of the surrounding waters, the accelerated gas transfer due to the stronger winds causes this anomalous source to be more strongly expressed. The net effect of this mesoscale correlation between wind speed and p_{CO_2} makes the ocean locally take up about 5–10% less CO_2 from the atmosphere. Although this is a small effect (see also ref. 21, based on monthly data), it may be of significance when considering that the Southern Ocean is globally the most important sink for anthropogenic CO_2 (ref. 22). In addition, with the eddies probably causing an anomaly of the air–sea CO_2 partial pressure difference of the order of 100%, eddies are a substantial source of variance for the Southern Ocean carbon sink. Finally, modification of mixing and Ekman pumping due to the coupling of winds and eddy currents could result in a modulation of biological productivity[23].

We have shown that transient mesoscale structures in the ocean can significantly alter atmospheric patterns introducing an oceanic mesoscale imprint in the atmosphere, disproving the common assumption of the atmosphere being independent of smaller-scale variability in the ocean. We suggest that air–sea interactions at the mesoscale may need to be considered in observational data analyses and numerical model simulations.

Methods

Data. Our analysis is based on satellite observations of oceanic and atmospheric properties: we analysed sea level anomalies from Aviso, SST, liquid cloud water and rain rates from AMSR-E (microwave radiometer), wind speeds from SeaWinds/QuikSCAT (microwave radar) and cloud fraction from GlobColour (see Supplementary Methods). Besides the rain rate we also looked at rain probability by assigning 0 to no-rain conditions and 1 to conditions of rain of any intensity.

The data were analysed at weekly resolution, which is long enough to largely filter out synoptic perturbations in the atmospheric data and are hence assumed to represent independent data points (Fig. 5 in ref. 24 and Supplementary Fig. S3). At the same time, this is sufficient to resolve the migration of eddies which is of O(10) km per week on average. The data are provided at a spatial resolution of 0.25° except for the sea level anomalies (1/3°; however, the feature resolution is coarser, owing to the processing of the observational data by the providers).

Eddy identification. We identified oceanic mesoscale eddies on the basis of sea level anomalies and the Okubo–Weiss parameter[13,14], which has been widely used for this purpose (for example, ref. 25). The Okubo–Weiss parameter separates areas of dominance of vorticity from areas of dominance of strain: $\mathrm{OW} = s_n^2 + s_s^2 - \omega^2$, where $s_n = u_x - v_y$ is the normal, $s_s = v_x + u_y$ is the shear component of the strain and $\omega = v_x - u_y$ is the relative vorticity. u and v are the current velocity components in the eastward and northward directions calculated from sea level anomalies under the assumption of geostrophy, and the subscripts x and y denote the partial derivatives in the eastward and northward directions, respectively. Vorticity dominates for $\mathrm{OW} < 0$. We used $\mathrm{OW} < -0.2\sigma_{\mathrm{OW}}$ as a threshold to determine the edge of the eddy core (as, for example, ref. 25), where σ_{OW} is the temporal mean of the spatial standard deviation of the Okubo–Weiss parameter. The eddy radius is defined as the radius of the core. The resulting eddy masks (with 1 for eddy and 0 for non-eddy) for each week were then linearly interpolated onto a 0.25° grid matching the atmospheric and SST data. We assigned all grid boxes containing a value greater than 0.5 to 1 (eddy) and below 0.5 to 0 (non-eddy). Cyclonic and anticyclonic eddies were separated depending on vorticity. We require an eddy to cover at least 4 adjacent grid boxes, reject shapes with a width of only a single grid box to avoid elongated features being detected as eddies, and only eddies detected in at least two consecutive time steps (see Supplementary Methods) are included in our analysis as robust features.

Definition of anomalies related to eddies. Anomalies of all quantities related to the oceanic eddies are calculated as differences of the respective quantity between the eddy-impact-area and the background. The former is defined as a circle of two radii around the centre of the eddy and the latter as a ring of three radii around this circle. The anomaly is defined as the difference of the mean of the two (used in Fig. 1 and Supplementary Figs S1, S2, S4, S6 and S7), except when interpreting the mean composite eddy (Fig. 2 and Supplementary Fig. S5) where we examine the maximum of the anomaly relative to the background.

Error and uncertainties. The error of the atmospheric quantities and SST for each individual eddy can easily be as large as the anomaly related to the individual eddy. The significance of our results arises from the large number of analysed eddies. A number of potential biases and errors need to be considered in more detail, however.

Our consideration of all eddies existing at least two weeks may cause a skewed result: the Aviso sea level anomalies were time filtered, which could lead to some frontal systems erroneously being classified as eddies. Another potential bias may stem from the assumption that the atmospheric data are decorrelated after one week. To test for the influence of these two effects, we analysed a case where we required all eddies to be at least 1 month old, and where we used the atmospheric data only from every other week. This entailed a reduction of the sample size by more than half but caused minor changes in the results and did not affect our conclusions: the patterns in the figures remained nearly the same (see Supplementary Figs S6–S9 in comparison with Figs 1 and 2 and Supplementary Figs S2 and S5). The error of the anomalies associated with eddies increased slightly (doubling at most) and a few more of the bins in Fig. 1 became insignificant (at $p = 0.01$) at the southern boundary and in the southern subtropical gyre in the Pacific where the least data are available (see Fig. 1a and Supplementary Fig. S6a).

SST is not available under rainy conditions and wind speed is subject to contamination by rain. The former is inconsequential as the decorrelation timescale of SST is typically longer than a week and therefore SST values a week before/after a rainy event are considered representative for the rain event also. Wind speed shows a positive bias with increasing rain rates at the wind and rain conditions of the Southern Ocean[26], which may inflate the signal we find in wind speeds related to eddies. Thus, we use only wind data without rain events for the calculation of correlations (Fig. 1 and Supplementary Figs S1, S4 and S6). Rain-free data are regarded as independent: these are derived making use of distinct spectral and polarization signatures in the microwave

brightness temperatures[27]. The bias of wind speed due to the change of water viscosity related to SST, and the deviation of actual winds from the equivalent neutral satellite winds, have been found to be small relative to the changes of winds due to atmospheric boundary layer adjustments in the course of SST anomalies[5,28].

Received 29 December 2012; accepted 28 May 2013; published online 7 July 2013

References

1. Hobbs, P. V. The Gulf Stream rainband. *Geophys. Res. Lett.* **14,** 1142–1145 (1987).
2. Minobe, S., Kuwano-Yoshida, A., Komori, N., Xie, S-P. & Small, R. J. Influence of the Gulf Stream on the troposphere. *Nature* **452,** 206–209 (2008).
3. White, W. B. & Annis, J. L. Coupling of extratropical mesoscale eddies in the ocean to westerly winds in the atmospheric boundary layer. *J. Phys. Oceanogr.* **33,** 1095–1107 (2003).
4. Chelton, D. B., Schlax, M. G., Freilich, M. H. & Milliff, R. F. Satellite measurements reveal persistent small-scale features in ocean winds. *Science* **303,** 978–983 (2004).
5. Park, K-A., Cornillon, P. & Codiga, D. L. Modification of surface winds near ocean fronts: Effects of Gulf Stream rings on scatterometer (QuikSCAT, NSCAT) wind observations. *J. Geophys. Res.* **111,** C03021 (2006).
6. Bryan, F. O. *et al*. Frontal scale air–sea interaction in high-resolution coupled climate models. *J. Clim.* **23,** 6277–6291 (2010).
7. Xie, S-P. Satellite observations of cool ocean–atmosphere interaction. *Bull. Amer. Meteorol. Soc.* **85,** 195–208 (2004).
8. O'Neill, L. W., Chelton, D. B., Esbensen, S. K. & Wentz, F. J. High-resolution satellite measurements of the atmospheric boundary layer response to SST variations along the Agulhas Return Current. *J. Clim.* **18,** 2706–2723 (2005).
9. Liu, W. T., Xie, X. & Niiler, P. P. Ocean–atmosphere interaction over Agulhas extension meanders. *J. Clim.* **20,** 5784–5797 (2007).
10. Xu, H., Xu, M., Xie, S-P. & Wang, Y. Deep atmospheric response to the spring Kuroshio over the East China Sea. *J. Clim.* **24,** 4959–4972 (2011).
11. Ferrari, R. & Wunsch, C. Ocean circulation kinetic energy: Reservoirs, sources, and sinks. *Annu. Rev. Fluid Mech.* **41,** 253–282 (2009).
12. Hausmann, U. & Czaja, A. The observed signature of mesoscale eddies in sea surface temperature and the associated heat transport. *Deep-Sea Res. Part I* **70,** 60–72 (2012).
13. Okubo, A. Horizontal dispersion of floatable particles in the vicinity of velocity singularities such as convergences. *Deep-Sea Res.* **17,** 445–454 (1970).
14. Weiss, J. The dynamics of enstrophy transfer in two-dimensional hydrodynamics. *Physica D* **48,** 273–294 (1991).
15. Spall, M. A. Midlatitude wind stress-sea surface temperature coupling in the vicinity of oceanic fronts. *J. Clim.* **20,** 3785–3801 (2007).
16. Small, R. *et al*. Air–sea interaction over ocean fronts and eddies. *Dyn. Atmos. Oceans* **45,** 274–319 (2008).
17. Chelton, D. B. & Xie, S-P. Coupled ocean–atmosphere interaction at oceanic mesoscales. *Oceanography* **23,** 52–69 (2010).
18. Iizuka, S. Simulations of wintertime precipitation in the vicinity of Japan: Sensitivity to fine-scale distributions of sea surface temperature. *J. Geophys. Res.* **115,** D10107 (2010).
19. Jin, X. *et al*. SST-wind interaction in coastal upwelling: Oceanic simulation with empirical coupling. *J. Phys. Oceanogr.* **39,** 2957–2970 (2009).
20. Shuckburgh, E. *et al*. Mixed layer lateral eddy fluxes mediated by air–sea interaction. *J. Phys. Oceanogr.* **41,** 130–144 (2011).
21. Wanninkhof, R., Park, G., Chelton, D. B. & Risien, C. M. in *Gas Transfer at Water Surfaces 2010* (eds Komori, S., McGillis, W. & Kurose, R.) 431–444 (Kyoto University Press, 2011).
22. Mikaloff Fletcher, S. E. *et al*. Inverse estimates of anthropogenic CO_2 uptake, transport, and storage by the ocean. *Glob. Biogeochem. Cycles* **20,** GB2002 (2006).
23. McGillicuddy, D. J. *et al*. Eddy/wind interactions stimulate extraordinary mid-ocean plankton blooms. *Science* **316,** 1021–1026 (2007).
24. O'Neill, L. W. Wind speed and stability effects on coupling between surface wind stress and SST observed from buoys and satellite. *J. Clim.* **25,** 1544–1569 (2012).
25. Isern-Fontanet, J., García-Ladona, E. & Font, J. Identification of marine eddies from altimetric maps. *J. Atmos. Ocean. Technol.* **20,** 772–778 (2003).
26. Hilburn, K. A., Wentz, F. J., Smith, D. K. & Ashcroft, P. D. Correcting active scatterometer data for the effects of rain using passive radiometer data. *J. Appl. Meteorol. Climatol.* **45,** 382–398 (2006).
27. Wentz, F. J. A well-calibrated ocean algorithm for special sensor microwave/imager. *J. Geophys. Res.* **102,** 8703–8718 (1997).
28. Liu, W., Xie, X. & Tang, W. in *Oceanography from Space: Revisited* (eds Barale, V., Alberotanza, L. & Gower, J.) Ch. 6, 93–111 (Springer Dordrecht Heidelberg, 2010).
29. Sallée, J. B., Speer, K. & Morrow, R. Response of the antarctic circumpolar current to atmospheric variability. *J. Clim.* **21,** 3020–3039 (2008).

Acknowledgements

The Center for Climate Systems Modelling (C2SM) at ETH Zürich provided financial support for this project.

Author contributions

I.F., M.M. and N.G. conceived the study, I.F. performed all analyses with support from M.M. R.K. provided support concerning statistical methods. All authors contributed to the interpretation and writing of the manuscript.

Additional information

Supplementary information is available in the online version of the paper. Reprints and permissions information is available online at www.nature.com/reprints. Correspondence and requests for materials should be addressed to I.F.

Competing financial interests

The authors declare no competing financial interests.